Iğdır Üniversitesi Fen Bilimleri Enstitüsü Dergisi, 12(1): 324-336, 2022
Journal of the Institute of Science and Technology, 12(1): 324-336, 2022

ISSN: 2146-0574, eISSN: 2536-4618

Kimya / *Chemistry* **DOI: 10.21597/jist.987744**

Araştırma Makalesi / *Research Article*

Geliş tarihi / Received: 27.08.2021 **Kabul tarihi / Accepted: 21.11.2021**

Atıf İçin: Bilgiç A, 2022. Schiff Bazlı Fonksiyonelleştirilmiş Yeni Sporopollenin Mikrokapsülün Sentezi ve Karakterizasyonu ve Cu (II)'nin Etkili Adsorpsiyonu için Kullanımı. Iğdır Üniversitesi Fen Bilimleri Enstitüsü Dergisi, 12(1): 324-336.

To Cite: Bilgiç A, 2022. Synthesis and Characterization of the Schiff Base-on Functionalized Novel Sporopollenin Microcapsule and Its Use for Effective Adsorption of Cu (II). Journal of the Institute of Science and Technology,12(1): 324-336.

Schiff Bazlı Fonksiyonelleştirilmiş Yeni Sporopollenin Mikrokapsülünün Sentezi ve Karakterizasyonu ve Cu(II)'nin Etkili Adsorpsiyonu için Kullanımı

Ali BİLGİÇ[1*]

ÖZET: Kanser ve karaciğer hasarı gibi ciddi hastalıklara neden olan Cu (II) iyonları özellikle su kirliliğinde önemli bir yere sahiptir. Bu ölümcül bakır (II) iyonlarını sulu çözeltiden etkin bir şekilde uzaklaştırmak için, adsorban olarak kullanılacak yeni işlevselleştirilmiş sporopollenin mikrokapsüllerinin (Sp-CPTS-HNMAA) sentezi amaçlandı. Sporopollenin yüzeyini işlevselleştirmek için kullanılan Schiff bazı (HNMAA), 2-Hidroksi-1-naftaldehit ve glisinin reaksiyonu sonucu elde edilmiş ve ^{1}H ve ^{13}C NMR ile karakterize edilmiştir. Sentezlenen Sp-CPTS-HNMAA mikrokapsül adsorbanı, FTIR, XRD ve SEM teknikleri ile başarılı bir şekilde karakterize edildi. Adsorpsiyon deneylerinde başlangıç Cu (II) konsantrasyonu, sıcaklık, pH, anyon, temas süresi ve adsorban dozunun etkileri araştırıldı. Adsorpsiyon dengesi, 150 dakikalık bir temas süresi, 30 mg L^{-1} başlangıç Cu (II) iyon konsantrasyonu, pH = 6 ve 0.03 g adsorban dozu ile maksimum Cu(II) giderimi ile % 92.73 olarak hesaplandı. Sp-CPTS-HNMAA mikrokapsül adsorbanının maksimum Cu (II) adsorpsiyon kapasitesi Langmuir izoterminden hesaplandı ve 32.57 mg g^{-1} olarak bulundu. Adsorpsiyon izotermi ve kinetik çalışmaları, Langmuir adsorpsiyon izotermine ve yalancı ikinci dereceden kinetik modele uyduğunu göstermiştir. Termodinamik çalışmaların sonuçları, adsorpsiyon reaksiyonunun tersinir, kendiliğinden ve endotermik olduğunu ve ayrıca Cu (II) iyonlarının Sp-CPTS-HNMAA üzerinde adsorpsiyonunun kimyasal bir adsorpsiyon işlemi olduğunu göstermiştir.

Anahtar Kelimeler: Sporopollenin, adsorpsiyon, termodinamik, Cu (II), mikrokapsül

Synthesis and Characterization of the Schiff Base-on Functionalized Novel Sporopollenin Microcapsule and Its Use for Effective Adsorption of Cu (II)

ABSTRACT: Cu (II) ions, which cause serious diseases such as cancer and liver damage, have an important place, especially in water pollution. To effectively remove these deadly copper (II) ions from aqueous solution, the synthesis of a new functionalized sporopollenin microcapsules (Sp-CPTS-HNMAA) to be used as an adsorbent was aimed. Schiff base (HNMAA), used to functionalize the surface of sporopollenin, was obtained as a result of the reaction of 2-Hydroxy-1-naphthaldehyde and glycine and was characterized by ^{1}H and ^{13}C NMR. The synthesized Sp-CPTS-HNMAA microcapsule adsorbent was successfully characterized by FTIR, XRD, and SEM techniques. The effects of initial Cu (II) concentration, temperature, pH, anion, contact time, and adsorbent dose were researched in adsorption experiments. The adsorption equilibrium was calculated as 92.73%, with a contact time of 150 min, initial Cu (II) ion concentration of 30 mg L^{-1}, pH = 6, and maximum Cu(II) removal with 0.03 g adsorbent dose. The maximum Cu (II) adsorption capacity of Sp-CPTS-HNMAA microcapsule adsorbent was calculated from the Langmuir isotherm and found to be 32.57 mg g^{-1}. Adsorption isotherm and kinetic studies indicated that it fits the Langmuir adsorption isotherm and pseudo-second-order kinetic model. The results of thermodynamic studies show that the adsorption reaction is reversible, spontaneous, and endothermic, and also showed that the adsorption of Cu (II) ions on Sp-CPTS-HNMAA is a chemical adsorption process.

Keywords: Sporopollenin, adsorption, thermodynamics, Cu (II), microcapsule

[1]Ali BİLGİÇ (**Orcid ID:** 0000-0002-7055-0847), Karamanoğlu Mehmetbey Üniversitesi, Teknik Bilimler Meslek Yüksekokulu, Mülkiyet Koruma ve Güvenlik Bölümü, Karaman, Türkiye

***Sorumlu Yazar/Corresponding Author:** Ali BİLGİÇ, e-mail: alibilgic@kmu.edu.tr

INTRODUCTION

Because of their toxicity, non-biodegradability, and bioaccumulation in living habitats, heavy metal pollution has become a global issue (Sutirman et al., 2020). Effluent discharges containing these heavy metal ions pose a severe danger to both the Earth's biological cycle and human health. One of these dangerous and widely distributed heavy metals is copper. Copper (Cu) is involved in many important industrial applications such as pulp production, fertilizer industries, sugar industry, jewelry making, alloys, kitchen appliances, war machines and weapons manufacturing, welding industry, and electrical wire construction, and it is also considered one of the elements that contribute to the activity of enzymes in the human body and engage in the metabolism and growth processes (Manzoor et al., 2019). Although the copper disclosed above is a very important element, its presence in high concentrations in water can cause deadly serious illnesses such as cancer and liver damage (Lavanya et al., 2017).

There are common conventional techniques used to remove copper or other heavy metals from water, such as reverse osmosis, chemical precipitation, ion exchange, solvent extraction, membrane filtration, etc., but these techniques are pricey and/or not fine for getting high removal efficiency (Gamal et al., 2021). Among these methods, the adsorption technique is widely utilized because of its high removal efficiency, wide application range, low cost, simplicity, and reusability (Yang et al., 2019; Tang et al., 2021a). Many natural adsorbents have been used to remove many different metal ions, including sporopollenin (Sp), from water. Sporopollenin (Sp) is a natural biopolymer that occurs in the outer membranes of fern and moss spores, as well as of most pollen grains (Chandrasekaram et al., 2021). The pollen and spore membranes of this biopolymer have been shown to have two layers; the outer part is known as exine containing a substance called sporopollenin, and the inner part is expressed as intine (Ünlü and Ersoz, 2007). It may survive millions of years in geological layers while retaining all of its morphological features, indicating that Sp is stable under severe circumstances (Gode and Pehlivan, 2007). The Sp's exact chemical structure is unknown. However, it has a stable cross-linked aromatic structure with hydrogen, oxygen, and carbon in a stoichiometry of $C_{90}H_{144}O_{27}$ (Ibrahim et al., 2020). The main functional group of Sp has hydroxyl functional groups existing for large amounts of modification, and this group serves as anchor sites for metal ion complexation as well as adding the desired surface functional groups and other materials with high affinity for the metal ion (Gürten et al. 2006; Ibrahim et al., 2020). However, the literature search shows that studies with Spropollenin microcapsule-based materials for the removal of metal ions are quite scarce. To the best of our knowledge, there exists no report on the use of sporopollenin microcapsule for the immobilization of HNMAA. The goal of this research was to investigate the Cu (II) adsorption performance of Sp-CPTS-HNMAA microcapsule adsorbents as a new adsorbent. For this purpose, the adsorption conditions of copper (II) ions were explored, and also the nature of the adsorption process in terms of isotherm, thermodynamic and kinetic aspects was evaluated.

MATERIALS AND METHODS

Chemicals and Instrumentation

The microcapsule (particle size 20 μm) of the L. clavatum sporopollenin, the starting support material of the prepared adsorbent, was provided from Sigma-Aldrich. 2-Hydroxy-1-naphthaldehyde, glycine (99%), petroleum ether (90%), copper (II) nitrate trihydrate (puriss. p.a., 99-104%), and 3-Chloropropyltrimethoxy silane (CPTS), were obtained from Sigma-Aldrich. Sodium hydroxide (≥98%), ethanol (99%), methanol (≥99.9%), acetone (99.5%), toluene (99.8%), and hydrochloric acid (37%)

were obtained from Merck (Darmstadt, Germany). Unless otherwise noted, all compounds utilized in the investigation were utilized without additional purification.

The FTIR spectra of the microcapsules and microcapsule adsorbent prepared in each step were scanned using a Perkin Elmer 100 FTIR spectrometer. XRD patterns of prepared microcapsules and microcapsule adsorbent were determined using a Bruker brand device (D8 Advance with Davinci). The surface morphologies of the pure sporopollenin (Sp), modified Sp-CPTS, and the Sp-CPTS-HNMAA microcapsule adsorbent was determined with the SEM apparatus (HITACHI (SU5000)). An NMR spectrometer (Varian 400 MHz) was used to record ^{1}H and ^{13}C NMR spectra measurements of the HNMAA compound. Cr (VI) ion concentrations remaining in the solutions were determined using Analytical Jena, Contr AA 300 brand flame atomic absorption spectrometry (FAAS).

Experimental Procedure

The synthesis of (Z)-2-(((2-hydroxynaphthalen-1-yl)methylene)amino)acetic acid (HNMAA): 0.172 g of 2-hydroxy-1-naphthaldehyde was added to a 150 mL reaction bottle containing 50 mL of methanol and dissolved by stirring for 10 min. Then 0.119 g of glycine dissolved in 30 ml of water was added to this solution. This mixture was refluxed for 3 h with constant stirring (Sevgi et al., 2018). After refluxing was complete, it was filtered. After 24 h, yellow crystals were obtained and recrystallized from methanol/petroleum ether. The synthesis of the HNMAA compound is shown in Figure 1.

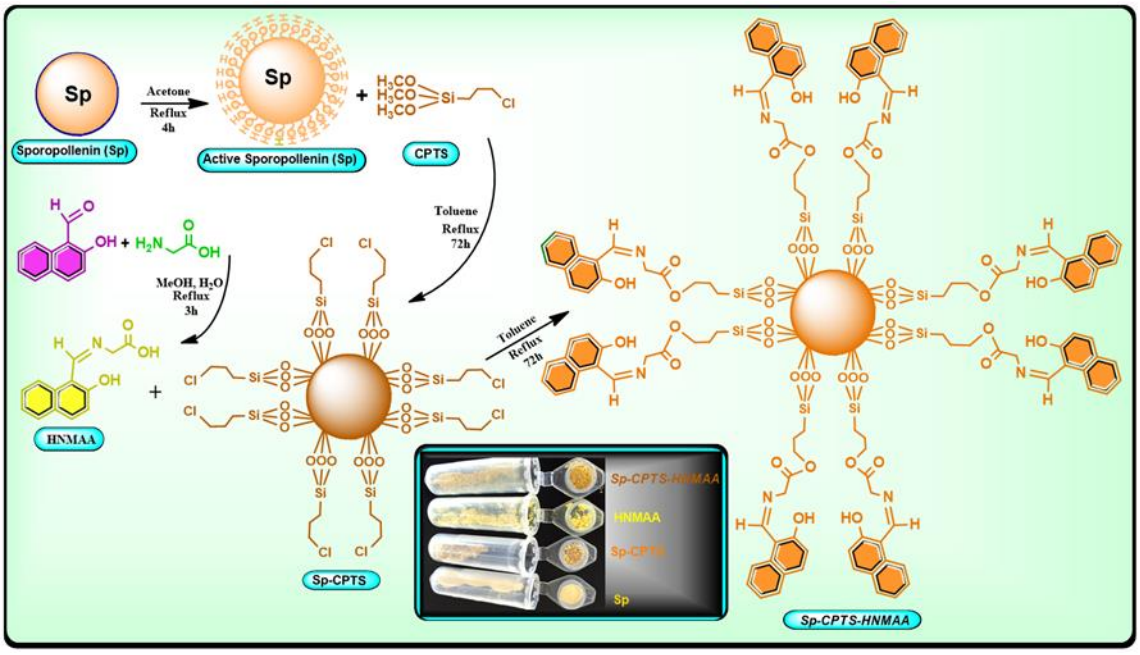

Figure 1. Schematic illustration of Sp, Sp-CPTS, Sp-CPTS-HNMAA, and HNMAA compound

The synthesis of Sp-CPTS-HNMAA microcapsule adsorbent: 100 mL of acetone and 5.0 g of sporopollenin were added to a 250 mL reaction vessel and the resulting suspension mixture was refluxed for 4 hours with continuous stirring (Gubbuk et al., 2012a). The suspension mixture was filtered, and the resulting active L. clavatum sporopollenin microcapsule was washed with pure water followed by methanol and then dried at 70 °C for 12 h. 5.0 g of active sporopollenin microcapsule was added into the reaction vessel containing 150 mL of anhydrous toluene, and he resultant mixture was stirred for 10 min at ambient temperature. Then (3-chloropropyl)triethoxysilane (CPTS) was added to this mixture and was refluxed for 72 h (Çimen et al., 2014; Gubbuk et al., 2021b). Sp-CPTS microcapsules were separated by filtration washed with $C_6H_5CH_3$, CH_3OH, and CH_3CH_2OH, and dried at 70 °C. In a 250 mL one-neck round-bottom flask, 5.0 g Sp-CPTS microcapsules were suspended in 100 mL anhydrous

toluene. Then 0.1 g of HNMAA compound was added to this mixture and stirred under reflux conditions for 72 h. After mixing was complete, the Sp-CPTS-HNMAA microcapsule adsorbent in suspension was separated by filtration, washed with $C_6H_5CH_3$, CH_3OH, and CH_3CH_2OH, and dried at 70 °C. The schematic route for the synthesis of the Sp-CPTS-HNMAA microcapsule adsorbent is given in Figure 1.

Batch Adsorption Experiments For Cu (II)

Cu (II) adsorption onto Sp-CPTS-HNMAA microcapsule adsorbent was carried out by batch adsorption process, and the influence of contact time, pH, temperature, adsorbent dose, anion, and initial copper concentration on adsorption was studied. The stock solution of copper (II) was prepared from 100 mg L^{-1} of $Cu(NO_3)_2 \cdot 3H_2O$ salt then diluted to the desired concentrations. Adsorption equilibrium studies were carried out by shaking 0.03 g of Sp-CPTS-HNMAA microcapsule adsorbent with 30 mL of copper (II) ion solutions of desired concentration at optimum conditions. Sp-CPTS-HNMAA microcapsule adsorbent was filtered from the suspension mixtures through filters (0.02 μm) at the end of the predetermined time interval. Then, the remaining copper ions in the solutions were measured by the FAAS. Each adsorption experiment was carried out with two replications to control calculations.

The following equation 1 and 2 were used to determine the amount of metal retained in the adsorbent phase (q_e, mg g^{-1}) and % Removal of metal ion, respectively, (Ali et al., 2016; Pavithra et al., 2021):

$$q_e = \frac{C_0 - C_e}{m}\, x\, V \quad (1)$$

$$\%\, Removal = \frac{C_0 - C_e}{C_e} x100 \quad (2)$$

Here, q_e (mg g^{-1}), V (L), C_e (mg L^{-1}), m (g), and C_0 (mg L^{-1}) are the equilibrium adsorption capacity, the volume of copper solution, the initial copper concentration, the weight of the adsorbent and equilibrium copper concentration, respectively.

RESULTS AND DISCUSSION

Characterization

FTIR and XRD analyses

The result of FTIR measurements for the natural sporopollenin (Sp), modified microcapsule (Sp-CPTS) and Sp-CPTS-HNMAA microcapsule adsorbent is shown in Figure 2a. In the FTIR spectrum of the sporopollenin microcapsule (Sp), the adsorption peaks observed at 3316 cm^{-1}, 2854-2925 $cm^{-1,}$ and 1709 cm^{-1} represent the hydroxyl (OH) (Ahmad et al., 2017), aliphatic (-CH, $-CH_2$, $-CH_3$) and carbonyl (C=O) groups, respectively (Dyab and Sadek, 2018). In the FTIR spectrum of the Sp-CPTS microcapsule, the two new absorption peaks at 1252 cm^{-1} and 693 cm^{-1} represent Si-C and C-CI groups in the Sp-CPTS microcapsule structure, respectively. The frequency of OH stretching vibration in Sp-CPTS is shifted to 3287 cm^{-1} from 3316 cm^{-1} (Sp). Other new peaks and shifts in the Sp-CPTS microcapsule's FTIR spectra show that the CPTS was modified to the sporopollenin's surface (Sp). In the FTIR spectrum of the Sp-CPTS-HNMAA microcapsule adsorbent, the absorption peaks at 1698 cm^{-1}, 1632 cm^{-1}, and 1496 cm^{-1} represent the –C=O stretching vibration of a carboxylic group, -C=N stretching vibrations, and the C=C stretching vibration of the aromatic rings, respectively. Also, the absorption peaks at 1343 cm^{-1} and 1194 cm^{-1} represent the stretching vibration of the C-O and the C-N bonds, respectively. In the FTIR spectrum of the Sp-CPTS-HNMAA microcapsule adsorbent, other new peaks and shifts show that the HNMAA compound was successfully immobilized to the Sp-CPTS surface.

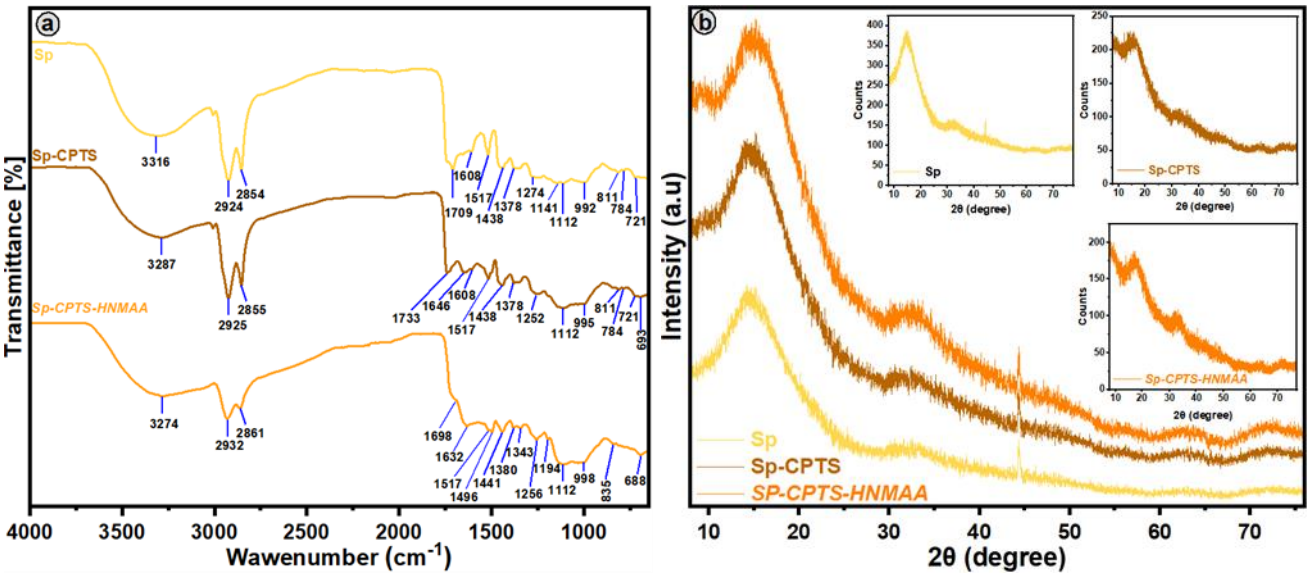

Figure 2. (a) FT-IR spectrum and (b) XRD patterns of the natural sporopollenin (Sp), Sp-CPTS, and the Sp-CPTS-HNMAA microcapsule adsorbent

The natural sporopollenin (Sp), modified microcapsule (Sp-CPTS), and the Sp-CPTS-HNMAA microcapsule adsorbent was investigated using XRD analysis, and the results are given in Figures 2b. The Natural L. clavatum sporopollenin microcapsules (Sp) (Figure 2b) showed a typical amorphous structure with a characteristic broad peak in the 25 - 8° range and about 15.24° (Sahin et al., 2012; Dyab and Sadek, 2018). In the XRD model of the Sp-CPTS (Figure 2b), the density of the characteristic sporopollenin peak was diminished. In the XRD model of the Sp-CPTS-HNMAA microcapsule adsorbent (Figure 2b), the intensity of the characteristic sporopollenin peak appears to be more reduced. These results approve that the characteristic structure of the sporopollenin is preserved, and the designed Sp-CPTS-HNMAA microcapsule adsorbent has been successfully synthesized.

^{1}H and ^{13}C NMR spectra of HNMAA compound; M.p.: 215 °C. ^{1}H-NMR [400 MHz, $CDCl_3$]: 13.71 (bs, OH) 13.07 (bs, COOH), 10.94 (s, HC=N), 8.2 (d, Ar-H), 7.88 (d, Ar-H), 7.74 (d, Ar-H), 7.45 (t, Ar-H), 7.22 (t, Ar-H), 6.71 (d, Ar-H), 4.41 (s, CH_2) ^{13}CNMR [100 MHz, d^{6}-DMSO]: δ (ppm) 52.2, 106.3, 118.8, 123.8, 126.2, 126.8, 128.8, 129.8, 135.7, 138.3, 160.3, 172.3, 177.4.

SEM analysis

To detect the morphological differences of the surface of the sporopollenin, it was characterized by Scanning electron microscopy (SEM), and the SEM images obtained are given in Figure 3a-c. As seen in the SEM image of the native L. clavatum sporopollenin microcapsules in Figure 3a, the surfaces of the microcapsules are smooth, pore structure (round microcapsule shape) and consist of a uniform hexagonal shape connected (Ahmad et al., 2017). The SEM image of Sp-CPTS in Figure 3b shows that the pores of the sporopollenin microcapsules are disrupted, and the surface is rough. Moreover, the SEM image of Sp-CPTS (Figure 3b) compared to the SEM image of the precursor natural microcapsules (Figure 3a) preserved the natural morphology of consistent size (approximately 25 μm in diameter) of the microcapsules. As seen in the SEM image of Sp-CPTS-HNMAA microcapsule adsorbent in Figure 3c, the pores of the microcapsules filled with HNMAA, and the pores became more rough and bumpy. The prepared Sp-CPTS-HNMAA microcapsule adsorbent confirms that it has been successfully synthesized according to these results.

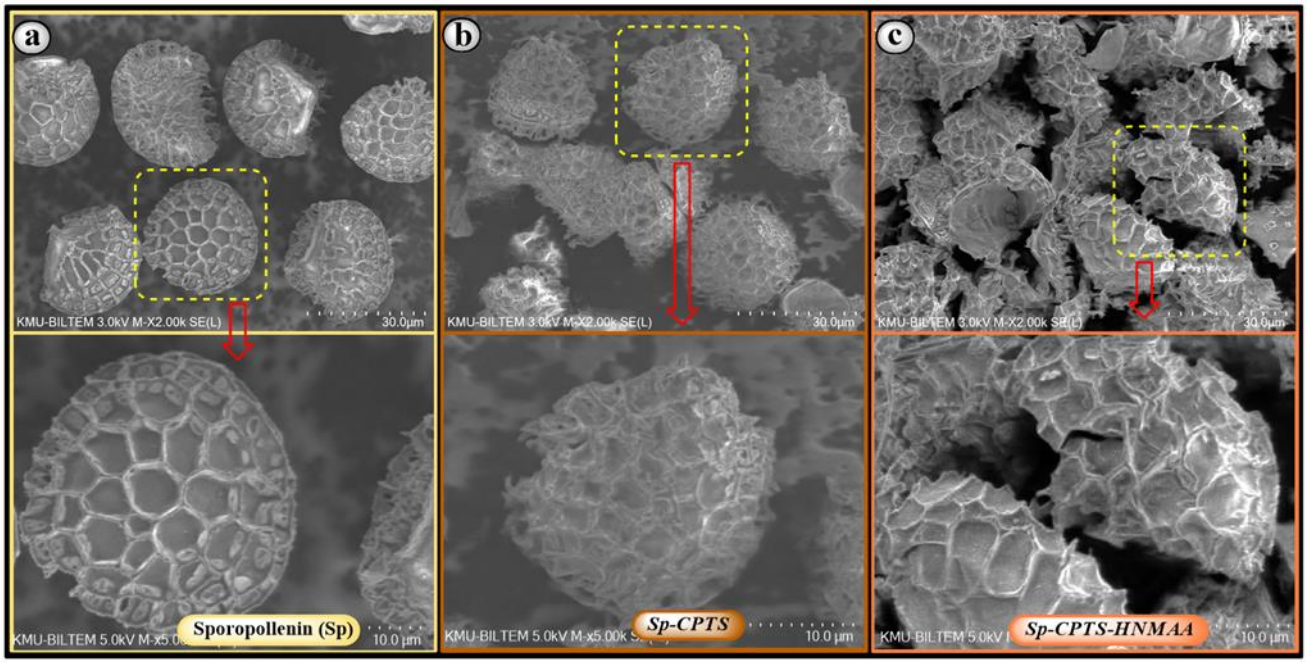

Figure 3. SEM microphotographs of (a) the natural sporopollenin (Sp), (b) Sp-CPTS, and (c) the Sp-CPTS-HNMAA microcapsule adsorbent

Adsorption Studies

Effect of microcapsule adsorbent dose and pH on adsorption

The influence of Sp-CPTS-HNMAA microcapsule adsorbent dose (in the range of (0.01 - 0.05 g) on the copper (II) adsorption by the Sp-CPTS-HNMAA microcapsule adsorbent was investigated (Vol of Cu (II) solution = 30 mL; copper (II) concentration = 30 mg L^{-1}; shaking speed = 250 rpm; temperature = 298 K, and contact time = 3 h.) and the results are given in Figure 4a. As shown in Figure 4a, in terms of general changes, Cu (II) removal efficiencies increased, and adsorption capacities of Sp-CPTS-HNMAA microcapsule adsorbents decreased with increasing Sp-CPTS-HNMAA microcapsule adsorbent dose. The increments in Cu(II) removal percentages can be attributed to the larger quantity of adsorption sites (the increased adsorbent surface area, active sites, pores, and the number of unsaturated sites) provided by the increasing Sp-CPTS-HNMAA microcapsule adsorbent dose (Nair et al., 2014; Tang et al., 2021b). However, the decrease in adsorption capacity (q_e) value with increasing adsorbent dose may be due to overlapping or aggregation of adsorption sites, thus reducing the total surface area available for the metal ion (Kayalvizhi et al., 2021). The number of metal ions adsorbed to the adsorbent unit mass decreases, causing the qe value to reduce as the adsorbent dose increases. Considering the removal efficiency and cost, the adsorbent dose of 0.03 g was selected and used in further studies.

The pH of the solution is one of the most important factors impacting the adsorption process. In this study, the influence of initial pH (1.0 - 7.0) on the removal percentage and adsorption capacity of Sp-CPTS-HNMAA microcapsule adsorbent against Cu (II) was investigated (Sp-CPTS-HNMAA microcapsule adsorbent dose = 0.03 g; vol of Cu (II) solution = 30 mL; contact time = 3 h; Cu (II) concentration= 30 mg L^{-1}; temperature = 298 K, and shaking speed = 250 rpm). Figure 4b depicts the results achieved. As seen in Figure 4b, the lowest adsorption efficiency (33%) and capacity (9.73 mg g^{-1}) were detected at pH 1. However, as the pH improved from 1 to 6, the adsorption capacity and efficiency were improved. At pH 6, the maximum adsorption capacity (27.67 mg g^{-1}) and efficiency (92.07%) were observed.

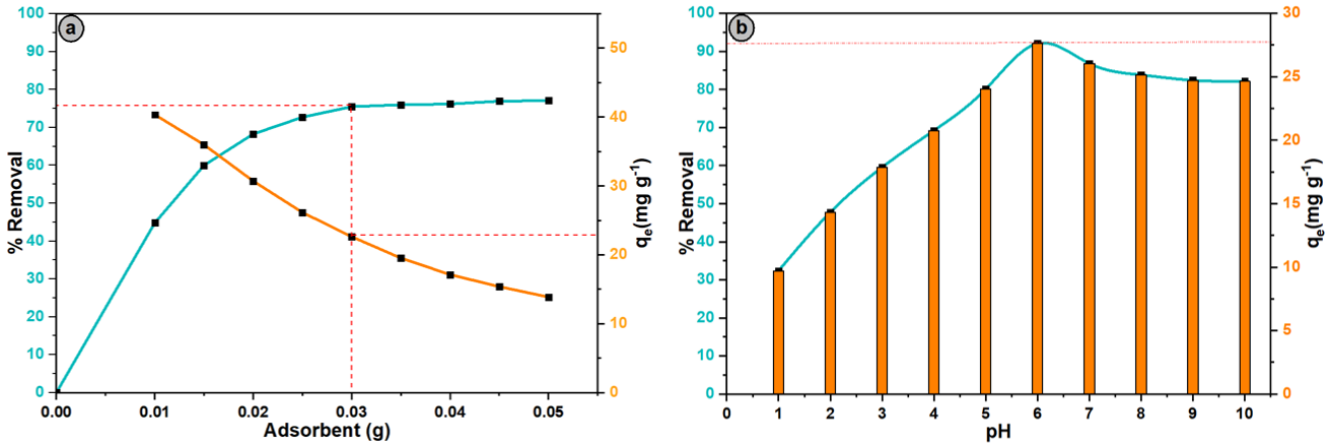

Figure 4. Influence of (a) Sp-CPTS-HNMAA microcapsule adsorbent dose and (b) pH on the adsorption of Cu (II) ions by the Sp-CPTS-HNMAA microcapsule adsorbent

Influence of contact time and initial concentration on Cu (II) adsorption

The influence of contact time on copper (II) adsorption by the Sp-CPTS-HNMAA microcapsule adsorbent was explored in the range of 5 - 300 min (Sp-CPTS-HNMAA microcapsule adsorbent dose = 0.03 g; vol of copper (II) solution = 30 mL; temperature = 298 K; pH = 6; Cu (II) concentration = 30 mg L^{-1}; and shaking speed = 250 rpm) and the obtained results are given in Figure 5a. As shown in Figure 5a, it is viewed that the adsorption efficiency and capacity of copper (II) ions increment with increasing time between 0 - 150 minutes and remain constant after this min (150 min).

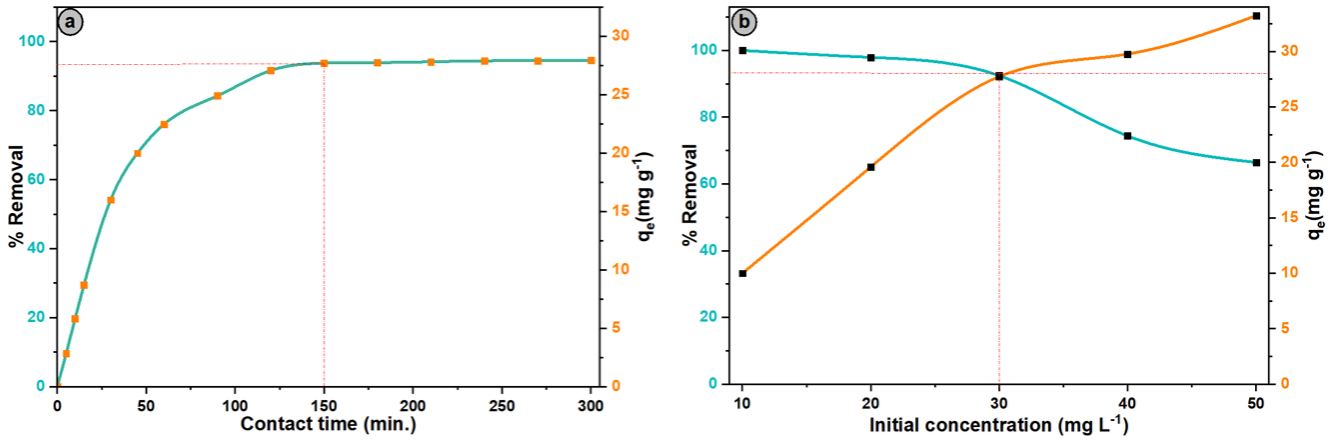

Figure 5. Effect of (a) contact time and (b) initial Cu (II) concentration on Cu (II) adsorption by the Sp-CPTS-HNMAA microcapsule adsorbent

The influence of initial Cu (II) concentration (10, 20, 30, 40 and 50 mg L^{-1}) on Cu (II) adsorption by the Sp-CPTS-HNMAA microcapsule adsorbents was investigated (Sp-CPTS-HNMAA microcapsule adsorbent dose = 0.03 g; vol of copper (II) solution = 30 mL; temperature = 298 K pH = 6 and shaking speed = 250 rpm) and the results are given in Figure 5b. As seen in Figure 5b, the removal percentage of Cu (II) decreased when the initial copper concentration was increased from 10 mg L^{-1} to 50 mg L^{-1}. On the other hand, it is seen that the adsorption capacity against increasing initial copper (II) ion concentration increases (Figure 5b). The initial concentration of copper (II) ion with the highest adsorption efficiency and capacity by the Sp-CPTS-HNMAA microcapsule adsorbent is 30 mg L^{-1}.

Adsorption isotherms

The adsorption isotherm gives important information about the adsorption capacity of the adsorbent and is also important in the optimization and design of the adsorption process (Sutirman et al., 2020). For this purpose, Temkin (Yu, 2020), Freundlich (Barbosa et al., 2018), Langmuir (Chen et al., 2021), and Dubinin-Radushkevich (Agarwal et al., 2021) isotherm models were applied to define the experimental data. The equations for these isotherm models are listed in Table 1. The graphs obtained from these equations are given in Figure 6(a-d), and the obtained isotherm parameters are shown in Table 1.

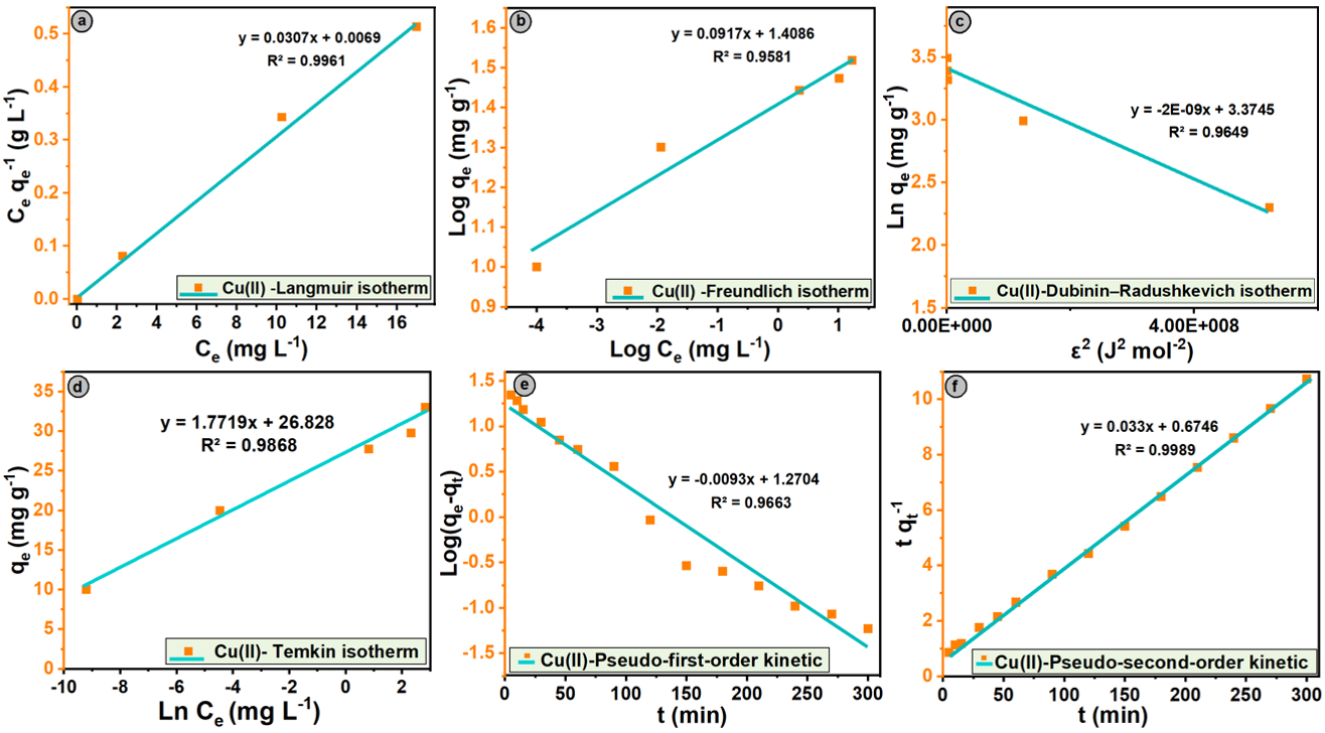

Figure 6. The plots of (a) Langmuir, (b) Freundlich, (c) Dubinin–Radushkevich, (d) Temkin, (e) Pseudo-first-order kinetic, and (f) Pseudo-second-order kinetic models

Table 1. Equations, parameter constants, and values of isotherm models

Models	Equation	Parameter constants	Parameter values
Langmuir	$C_e/q_e = (C_e/q_m) + (1/(K_L q_m))$	q_m ((mg g^{-1})	32.57
		b (L mg^{-1})	4.449
		R^2	0.9961
	$R_L = 1 / [1+ (K_L . C_o)]$	R_L	0.002 - 0.004
Freundlich	$Logq_e = logK_F + (1/n)logC_e$	n	10.905
		1 n^{-1}	0.0917
		K_F (mg g^{-1})	4.090
		R^2	0.9581
Dubinin - Radushkevich (D-R)	$Lnq_e = lnq_{D-R} - K_{ad}\varepsilon^2$	q_{D-R} (mg g^{-1})	29.297
	$\varepsilon = RTln(1+(1/C_e))$	K_{D-R} (mol^2 J^{-2})	0.02x10^{-7}
	$E = (2K_{ad})^{-1/2}$	R^2	0.9649
		E (KJ mol^{-1})	15.811
Temkin	$qe = (RT/b_T)lnA_T + (RT/b_T)ln\ C_e$	b_T (kJ mol^{-1})	1.544
		A_T (L g^{-1})	3.7 x10^6
		R^2	0.9868

As shown in Table 1, since the R^2 value of the Langmuir model is higher than the other three models, we can say that the adsorption process fits the Langmuir isotherm. Its suitability for the Langmuir isotherm indicates the formation of monolayer coverage on surface of the Sp-CPTS-HNMAA

microcapsule adsorbent of Cu (II) ions. Also, R_L values (0.022 - 0.004) is in the range of 0 to 1, which means that the adsorption of copper (II) ions onto the Sp-CPTS-HNMAA microcapsule adsorbent is appropriate under the operating conditions used in this work. Since the E value (15.811 kJ mol^{-1}) calculated from the D-R isotherm model is in the range of 8 - 16 kJ mol^{-1}, it was concluded that the adsorption of Cu (II) ions on Sp-CPTS-HNMAA microcapsule adsorbent was realized by chemical ion exchange (Tural et al., 2018).

Adsorption kinetics

Adsorption kinetics were studied to explain the adsorption mechanism of copper (II) ions on Sp-CPTS-HNMAA microcapsule adsorbent and the associated rate-limiting steps. To examine the adsorption kinetics, widely used pseudo-second-order kinetic and pseudo-first-order models were analyzed (Ge et al., 2017). Equations ((3) and (4)) of these kinetic models are as follows, respectively.

$$\frac{t}{q_t} = \frac{1}{k_2 q_e 2} + \frac{t}{q_e} \quad (3)$$

$$\log(q_e - q_t) = \log q_e - \frac{t.k_1}{2.303} \quad (4)$$

The data obtained regarding the influence of contact time on adsorption of Cu (II) ions by the Sp-CPTS-HNMAA microcapsule adsorbent were fitted to these models, and the graphs and kinetic parameters of the results obtained are given in Figure 6 (e and f) and Table 2, respectively. As can be seen from the correlation coefficient (R^2) values in Table 2, the adsorption kinetics fits better the pseudo-second-order model (R^2 = 0.9989). Also, the value of qe (27,782 mg g^{-1}) obtained in the experimental value is consistent with the value of qe (30.303 mg g^{-1}) calculated from the pseudo-second-order model. These findings show that the adsorption process fits the pseudo-second model, and it can be concluded that the copper (II) adsorption by the Sp-CPTS-HNMAA microcapsule adsorbent is related to the chemical interaction (Ge et al., 2014).

Table 2. Calculated thermodynamic and adsorption kinetic parameters

Kinetic model	Parameter	Cu (II)	Thermodynamic parameters		Cu(II)
	R^2	0.9663	ΔH^o (kJ mol^{-1})		36.712
Pseudo-first-order	k_1(1 min^{-1})	0.0214	ΔS^o (J K mol^{-1})		143.151
	q_e (mg g^{-1})	18.638	R^2		0.9691
				298 (K)	-5.968
	k_2 (g mg^{-1} min^{-1})	0.001		308(K)	-7.399
Pseudo-second-order	R^2	0.9989	ΔG^o (kJ mol^{-1})	318 (K)	-8.831
	q_e (mg g^{-1})	30.303		328 (K)	-10.263

Effect of temperature and thermodynamic studies

The influence of temperature on copper adsorption by the Sp-CPTS-HNMAA microcapsule adsorbent was investigated in the range of 298 K to 328 K (Sp-CPTS-HNMAA microcapsule dose = 0.03 g; pH = 6; vol of copper (II) solution = 30 mL; Cu (II) concentration = 30 mg L^{-1} and shaking speed = 250 rpm) and the results are given in Figure 7a. As seen in Figure 7a, it is seen that as the temperature of the suspension solution increases, the adsorption efficiency and capacity of Cu (II) ions slightly increase, indicating that the adsorption process of copper ions by the Sp-CPTS-HNMAA microcapsule adsorbent is endothermic in nature. To analyze the thermodynamic nature of Cu (II) adsorption on Sp-CPTS-HNMAA microcapsule adsorbent, the data from the influence of temperature on adsorption were applied to the following equations ((5), (6) and (7)) (El-Massaoudi et al., 2021).

$$\Delta G° = -RT\ln K_d \quad (5)$$

$$\Delta G° = \Delta H° - T\Delta S° \quad (6)$$

$$\ln K_d = (\Delta S°/R) - (\Delta H°/RT) \quad (7)$$

Van't Hoff plot obtained from Equation 7 is given in Figure 7b, and the thermodynamic parameters obtained from these equations are listed in Table 2. As seen in Table 2, the positive enthalpy (ΔH°) value (36.712 kJ mol^{-1}) demonstrates that the adsorption process is endothermic. At the same time, the enthalpy (ΔH°) value (36.712 kJ mol^{-1}) was greater than 20 kJ mol^{-1}, which proved that the adsorption performed in this study is a chemical adsorption process (Bartell et al., 1951; Tang et al., 2021). The Gibbs free energy (ΔG°) is negative values at different temperatures, indicating that Sp-CPTS-HNMAA microcapsule adsorbent can spontaneously adsorb Cu (II) ions. In addition, the Gibbs free energy (ΔG°) value reduces as the temperature increments, indicating that the adsorption on Sp-CPTS-HNMAA microcapsules of Cu (II) ions is easier under high-temperature conditions (Zhang et al., 2019). The positive value of entropy (ΔS°) is a result of the increment in randomness at the solid-liquid interface. In addition, since the obtained entropy (ΔS°) value (143.151 J $K^{-1}mol^{-1}$) is greater than -10 J $K^{-1}mol^{-1}$, it shows that the copper adsorption involves a dissociative adsorption mechanism (Akpomie et al., 2015; Ahmad and Mirza, 2017).

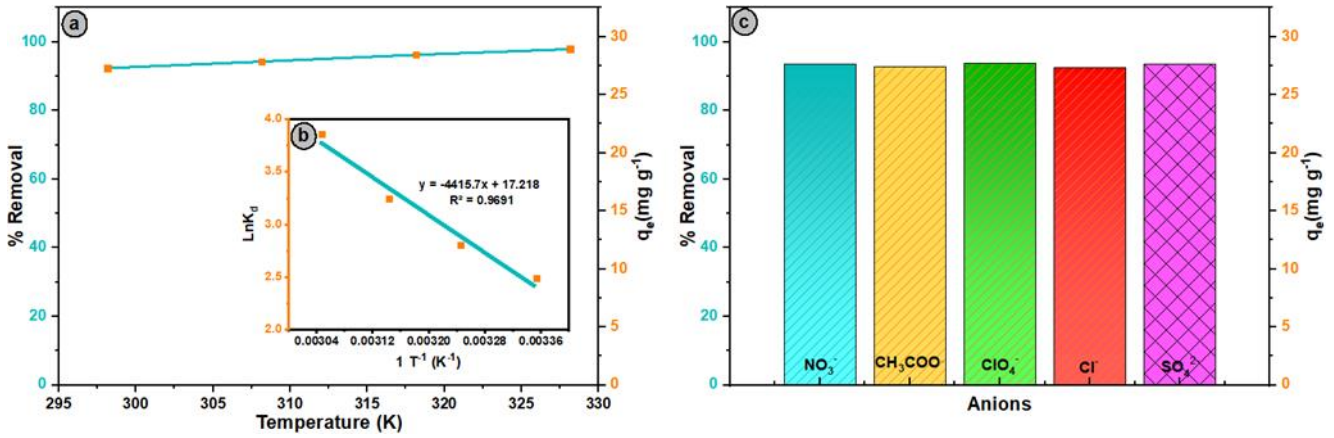

Fig. 7. (a) Influence of temperature on Cu (II) adsorption by the Sp-CPTS-HNMAA microcapsule adsorbent, (b) Van't Hoff plot for the removal of Cu (II) ions by the Sp-CPTS-HNMAA microcapsule adsorbent, and (c) Effect of the anions (NO_3^-, CH_3COO^-, ClO_4^-, Cl^- and SO_4^{2-}) on the adsorption of Cu (II) ions by the Sp-CPTS-HNMAA microcapsule adsorbent

Effect of the anions (NO_3^-, CH_3COO^-, ClO_4^-, Cl^- and SO_4^{2-})

Based on the above adsorption experiments, the influence of different anions (NO_3^-, CH_3COO^-, ClO_4^-, Cl^- and SO_4^{2-}) on copper adsorption by the Sp-CPTS-HNMAA microcapsule adsorbent under the same conditions (Sp-CPTS-HNMAA microcapsule dose = 0.03 g; temperature = 298 K; contact time = 150 min; vol of Cu (II) solution = 30 mL; pH = 6; Cu (II) concentration = 30 mg L^{-1}; and shaking speed = 250 rpm) was investigated. The results obtained are demonstrated in Figure 7(c). As seen in Figure 7(c), the removal percentage and adsorption capacity of copper (II) ions were approximately the same in the asset of different anions. Different anions have no important effect on Cu (II) adsorption. Therefore, there is a strong bond between adsorbate (copper (II)) and adsorbent (Sp-CPTS-HNMAA) (Wang et al., 2018; Mu et al., 2020).

CONCLUSION

In this study, environmentally friendly Sp-CPTS-HNMAA microcapsule adsorbents were prepared for the effective removal of Cu (II) ions from aqueous solutions. Sp-CPTS-HNMAA microcapsule adsorbent was characterized by SEM, FTIR, and XRD analysis and confirmed that it was successfully synthesized. In adsorption studies, the equilibrium time is 150 min, and the maximum adsorption is at optimum pH = 6. Thermodynamic parameters were derived from the effect of

temperature, and positive ΔH° and ΔS° values demonstrated that the adsorption process was endothermic and reversible, while negative ΔG° values demonstrated that adsorption was spontaneous. The Dubinin - Radushkevich, Temkin, Freundlich, and Langmuir isotherm models were used in the adsorption isotherm calculations, and the Langmuir model was determined to have the best fit. The maximum adsorption capacity calculated according to the Langmuir model is 32.57 mg g^{-1}. The adsorption kinetics fit the pseudo-second-order model. All these results show that the synthesized Sp-CPTS-HNMAA microcapsule adsorbent has great potential; it can be concluded that it is low cost, environmentally friendly, can remove Cu (II) effectively, and is promising and efficient.

Conflict of Interest

The author declares that this research article has no conflict of interest.

Author's Contributions

I declare that the planning, execution, and writing of this research article were done by me as the sole author of the manuscript.

REFERENCES

Agarwal A, Kumar A, Gupta P, Tomar R, Singh NB, 2021. Cu (II) ions removal from water by charcoal obtained from marigold flower waste. Materials Today: Proceedings, 34:875-879.

Ahmad NF, Kamboh MA, Nodeh HR, Abd Halim SNB, Mohamad S, 2017. Synthesis of piperazine functionalized magnetic sporopollenin: a new organic-inorganic hybrid material for the removal of lead (II) and arsenic (III) from aqueous solution. Environmental Science and Pollution Research, 24(27):21846-21858.

Ahmad R, Mirza A, 2017. Adsorption of Pb (II) and Cu (II) by Alginate-Au-Mica bionanocomposite: kinetic, isotherm, and thermodynamic studies. Process Safety and Environmental Protection, 109:1-10.

Akpomie KG, Dawodu FA, Adebowale KO, 2015. Mechanism on the sorption of heavy metals from binary-solution by a low cost montmorillonite and its desorption potential. Alexandria Engineering Journal, 54(3):757-767.

Ali RM, Hamad HA, Hussein MM, Malash GF, 2016. Potential of using green adsorbent of heavy metal removal from aqueous solutions: adsorption kinetics, isotherm, thermodynamic, mechanism and economic analysis. Ecological Engineering, 91:317-332.

Barbosa TR, Foletto EL, Dotto GL, Jahn SL, 2018. Preparation of mesoporous geopolymer using metakaolin and rice husk ash as synthesis precursors and its use as potential adsorbent to remove organic dye from aqueous solutions. Ceramics International, 44(1):416-423.

Bartell FE, Thomas TL, Fu Y, 1951. Thermodynamics of adsorption from solutions. IV. Temperature dependence of adsorption. The Journal of Physical Chemistry, 55(9):1456-1462.

Chandrasekaram K, Alias Y, Fathullah SF, Lee VS, Haron N, Raoov M, Mohamad S, 2021. Sporopollenin supported ionic liquids biosorbent for enhanced selective adsorption of 2, 4-dinitrophenol from aqueous environment. Materials Today Communications, 28:102587.

Chen Y, Cui J, Liang Y, Chen X, Li Y, 2021. Synthesis of magnetic carboxymethyl cellulose/graphene oxide nanocomposites for adsorption of copper from aqueous solution. International Journal of Energy Research, 45(3):3988-3998.

Çimen A, Bilgiç A, Kursunlu AN, Gübbük, İH, Uçan Hİ, 2014. Adsorptive removal of Co(II), Ni(II), and Cu(II) ions from aqueous media using chemically modified sporopollenin of Lycopodium clavatum as novel biosorbent. Desalination and Water Treatment, 52(25-27):4837-4847.

Dyab AK, Sadek KU, 2018. Microwave assisted one-pot green synthesis of cinnoline derivatives inside natural sporopollenin microcapsules. RSC Advances, 8(41):23241-23251.

El-Massaoudi M, Radi S, Lamsayah M, Tighadouini S, Séraphin KK, Kouassi LK, Garcia Y, 2021. Ultra-fast and highly efficient hybrid material removes Cu (II) from wastewater: Kinetic study and mechanism. Journal of Cleaner Production, 284:124757.

Gamal A, Ibrahim AG, Eliwa EM, El-Zomrawy AH, El-Bahy SM, 2021. Synthesis and characterization of a novel benzothiazole functionalized chitosan and its use for effective adsorption of Cu (II). International Journal of Biological Macromolecules, 183:1283-1292.

Ge Y, Cui X, Liao C, Li Z, 2017. Facile fabrication of green geopolymer/alginate hybrid spheres for efficient removal of Cu (II) in water: Batch and column studies. Chemical Engineering Journal, 311:126-134.

Ge Y, Xiao D, Li Z, Cui X, 2014. Dithiocarbamate functionalized lignin for efficient removal of metallic ions and the usage of the metal-loaded bio-sorbents as potential free radical scavengers. Journal of Materials Chemistry A, 2(7):2136-2145.

Gode F. Pehlivan E, 2007. Sorption of Cr(III) onto chelating b-DAEG–sporopollenin and CEP–sporopollenin resins. Bioresource Technology, 98:904-911.

Gubbuk IH, Gürfidan L, Erdemir S, Yilmaz M. 2012b. Surface modification of sporopollenin with calixarene derivative. Water, Air, & Soil Pollution, 223(5):2623-2632.

Gubbuk IH, Ozmen M, Maltas E. 2012a. Immobilization and characterization of hemoglobin on modified sporopollenin surfaces. International Journal of Biological Macromolecules, 50(5): 1346-1352.

Gürten AA, Uçan M, Abdullah MI, Ayar A, 2006. Effect of the temperature and mobile phase composition on the retention behavior of nitroanilines on ligand-exchange stationary phase. Journal of hazardous materials, 135(1-3):53-57.

Ibrahim WAW, Hassan AAM, Sutirman ZA, Bakar MB, 2020. A mini review on sporopollenin-based materials for removal of heavy metal ions from aqueous solution. Malaysian Journal of Analytical Sciences, 24(3):300-312.

Kayalvizhi K, Alhaji NMI, Saravanakkumar D, Mohamed SB, Kaviyarasu K, Ayeshamariam A, Elshikh MS, 2021. Adsorption of copper and nickel by using sawdust chitosan nanocomposite beads–A kinetic and thermodynamic study. Environmental Research, 203:111814.

Lavanya R, Gomathi T, Vijayalakshmi K, Saranya M, Sudha PN, Anil S, 2017. Adsorptive removal of copper (II) and lead (II) using chitosan-g-maleic anhydride-g-methacrylic acid copolymer. International journal of biological macromolecules, 104:1495-1508.

Manzoor K, Ahmad M, Ahmad S, Ikram S, 2019. Synthesis, characterization, kinetics, and thermodynamics of EDTA-modified chitosan-carboxymethyl cellulose as Cu (II) ion adsorbent. ACS omega, 4(17):17425-17437.

Mu, R, Liu, B, Chen, X, Wang, N, Yang, J, 2020. Adsorption of Cu (II) and Co (II) from aqueous solution using lignosulfonate/chitosan adsorbent. International Journal of Biological Macromolecules, 163:120-127.

Nair V, Panigrahy A, Vinu R, 2014. Development of novel chitosan–lignin composites for adsorption of dyes and metal ions from wastewater. Chemical Engineering Journal, 254:491-502.

Pavithra S, Thandapani G, Sugashini S, Sudha PN, Alkhamis HH, Alrefaei AF, Almutairi MH, 2021. Batch adsorption studies on surface tailored chitosan/orange peel hydrogel composite for the removal of Cr (VI) and Cu (II) ions from synthetic wastewater. Chemosphere, 271:129415.

Sahin M, Gubbuk IH, Kocak N, 2012. Synthesis and characterization of sporopollenin-supported schiff bases and ruthenium (III) sorption studies. Journal of Inorganic and Organometallic Polymers and Materials, 22(6):1279-1286.

Sevgi, F, Bagkesici U, Kursunlu AN, Guler E, 2018. Fe (III), Co (II), Ni (II), Cu (II) and Zn (II) complexes of schiff bases based-on glycine and phenylalanine: Synthesis, magnetic/thermal properties and antimicrobial activity. Journal of Molecular Structure, 1154:256-260.

Sutirman ZA, Rahim EA, Sanagi MM, Abd Karim KJ, Ibrahim WAW, 2020. New efficient chitosan derivative for Cu (II) ions removal: characterization and adsorption performance. International Journal of Biological Macromolecules, 153:513-522.

Tang CJ, Chen X, Feng F, Liu ZG, Song YX, Wang YY, Tang X, 2021b. Roles of bacterial cell and extracellular polymeric substance on adsorption of Cu (II) in activated sludges: A comparative study. Journal of Water Process Engineering, 41:102094.

Tang L, Gou S, He Y, Liu L, Fang S, Duan W, Liu T, 2021a. An efficient chitosan-based adsorption material containing phosphoric acid and amidoxime groups for the enrichment of Cu (II) and Ni (II) from water. Journal of Molecular Liquids, 331:115815.

Tural S, Ece MŞ, Tural B, 2018. Synthesis of novel magnetic nano-sorbent functionalized with N-methyl-D-glucamine by click chemistry and removal of boron with magnetic separation method. Ecotoxicology and environmental safety, 162:245-252.

Ünlü N, Ersoz M, 2007. Removal of heavy metal ions by using dithiocarbamated-sporopollenin. Separation and Purification Technology, 52(3):461-469.

Wang, Y, Wang, X, Ding, Y, Zhou, Z, Hao, C, Zhou, S, 2018. Novel sodium lignosulphonate assisted synthesis of well dispersed Fe_3O_4 microspheres for efficient adsorption of copper (II). Powder Technology, 325:597-605.

Yang H, Bai L, Wei D, Yang L, Wang W, Chen H, Xue Z, 2019. Ionic self-assembly of poly (ionic liquid)-polyoxometalate hybrids for selective adsorption of anionic dyes. Chemical Engineering Journal, 358, 850-859.

Yu Z, Song W, Li J, Li Q, 2020. Improved simultaneous adsorption of Cu (II) and Cr (VI) of organic modified metakaolin-based geopolymer. Arabian Journal of Chemistry, 13(3):4811-4823.

Zhang H, Omer AM, Hu Z, Yang LY, Ji C, Ouyang XK, 2019. Fabrication of magnetic bentonite/carboxymethyl chitosan/sodium alginate hydrogel beads for Cu (II) adsorption. International journal of biological macromolecules, 135:490-500.